A single-domain antibody detects $A\beta_{42}$ oligomers and prevents their associated neurotoxicity*

Irem Kural[1,2], Liliana Napolitano[2] and Roberta Cascella[2]

[1]Hasselt University, Biomedical Research Institute, BIOMED, Campus Diepenbeek, Agoralaan Gebouw C - B-3590 Diepenbeek
[2]Department of Experimental and Clinical Biomedical Sciences, Section of Biochemistry, University of Florence, Florence, Italy

*Running title: *A single-domain antibody against toxic $A\beta_{42}$ oligomers*

To whom correspondence should be addressed: Roberta Cascella, Tel: +390 552 751 223; Email: roberta.cascella@unifi.it

Keywords: Conformation-sensitive antibodies, Oligomers, Neurotoxicity, Amyloid-beta42, Alzheimer's disease

ABSTRACT

Alzheimer's disease (AD) poses a global challenge due to its rising prevalence and lack of preventive measures, effective therapies, or early diagnostic tests. Soluble amyloid-β42 ($A\beta_{42}$) oligomers are considered as the primary agents behind neurotoxicity in AD pathogenesis. Single-domain antibodies (sdAbs) hold promise for precise diagnosis as well as therapeutic intervention. In this work, we characterised $A\beta_{42}$ aggregation, assessing morphology and cytotoxicity on neuronal cells using thioflavin T, dot blot, and STED microscopy. Moreover, we evaluated the effectiveness of a sdAb, named DesAb-O, in neutralising oligomer-induced cell dysfunction and oxidative stress, and in selectively binding to oligomers, through MTT assays, confocal microscopy, dot blot and ELISA assays. Our results revealed well-resolved $A\beta_{42}$ aggregates, including oligomers and fibrils, with varying cytotoxic properties. Notably, DesAb-O demonstrated the ability to mitigate $A\beta_{42}$-induced mitochondrial dysfunction and oxidative stress through selective binding to the oligomers with respect to monomers and fibrils. Overall, our study reveals the ability of DesAb-O to specifically target toxic $A\beta_{42}$ oligomers, indicating sdAbs as promising tools for AD diagnostics and therapeutics, thus contributing to advancements in early AD diagnosis and treatment to mitigate its impact worldwide.

INTRODUCTION

As the most prominent form of dementia, Alzheimer's disease (AD) poses a significant challenge in the field of neurological disease, creating a substantial burden on affected individuals. Nowadays, ca. 60-70% of 55 million people worldwide suffer from AD (Alzheimer's association, 2023). Furthermore, researchers from the Institute for Health Metrics and Evaluation at the University of Washington School of Medicine, as reported at AAIC 2021, anticipate a rise in dementia cases, estimating that the number of affected people will nearly triple to exceed 152 million by 2050 (1, 2). Given the sharp increase of AD cases, the demand for precise and early diagnostic tools has become increasingly urgent. This urgency is underscored by the progressive nature of AD, where interventions in the early stages hold significant promise for improved outcomes (3). Unlike the normal brain, the AD brain generally shows neural cell death induced by the accumulation of extracellular amyloid-beta (Aβ) plaques and intracellular tau neurofibrillary tangles in neurons, leading to synapse loss and cognitive decline (4-5). Aβ plaques, formed through a complex aggregation process involving species with different structural and biological properties, consist primarily of aggregated forms of the Aβ peptide. In the last decades, accumulating evidences strongly implicate small, soluble oligomers of the 42-residue form of Aβ ($A\beta_{42}$), formed early during the aggregation process or released from mature fibrils, as the primary agents

responsible for neurotoxicity in AD pathogenesis (6-9). Numerous methods have been investigated to elucidate the structural determinants contributing to the neurotoxicity of oligomers (10). Among these determinants, both size and hydrophobic exposure play crucial roles in the activation of various cytotoxic pathways. These cellular processes include membrane disruption and permeabilization, oxidative stress, alteration of mitochondrial functionality, synaptic dysregulation and activation of proinflammatory response, ultimately resulting in neuronal death (6-9, 11).

Elevated oligomer levels have been detected in AD patients and are known to correlate stronger with the severity of cognitive decline and with the loss of synaptic markers compared to mature fibrils (12, 13). Furthermore, soluble Aβ oligomers have been recently indicated to be elevated within the cerebrospinal fluid (CSF) of AD patients compared to age-matched controls (14, 15). However, the transient and heterogeneity properties of these neurotoxic aggregates have determined the lack of suitable sensitive methods for their detection, quantification and isolation from biological fluids.

In the last few years, the advancement in developing conformation-specific Abs against the more toxic $A\beta_{42}$ oligomers has paved the way for a more precise form of diagnosis (15-16). Several monoclonal antibodies (mAbs), targeting specific forms of $A\beta_{42}$, have been developed to bind and remove Aβ (17). Unfortunately, they were found only to slow down AD decline without inhibiting it completely or reverting it (18-20).

The challenging detection of small soluble protein aggregates to reduce their toxicity could be an important strategy against AD. In this context, nanobodies or single-domain Abs (sdAbs) could represent a real step forward for the early diagnosis of AD, but also for therapy (21). Described as recombinant, antigen-specific variable fragments derived from camelid heavy chain-only Abs, sdAbs make great candidates for diagnostic and therapeutic applications due to their small size, solubility and low immunogenicity (22, 23). In particular, previously published works (24, 25) demonstrated that targeting the region 29 to 36 of $A\beta_{42}$ with rationally designed Abs, called DesAbs, can interfere with Aβ aggregation process (26, 27). Among these DesAbs, DesAb-O was found to preferentially bind to Aβ oligomers rather than its monomeric and fibrillar forms, as this region is likely to be solvent-exposed when the peptide is oligomeric, before becoming buried in amyloid fibrils (25). Furthermore, DesAb-O is able to selectively detect synthetic $A\beta_{42}$ oligomers both *in vitro* and in cultured cells, and to neutralise their associated neuronal dysfunction (21). DesAb-O can also identify $A\beta_{42}$ oligomers present in the CSFs of AD patients with respect to healthy individuals (21).

In this study, we first characterised the reactive properties and the morphology of diverse and heterogeneous $A\beta_{42}$ aggregates obtained from Thioflavin T (ThT) aggregation assays and we monitored their cytotoxic effects. We took advantage of an array of well-established biochemical and cell biological methods, such as dot blot assays, stimulated emission-depletion super resolution (STED) microscopy and MTT reduction assays on human SH-SY5Y neuroblastoma cells. Furthermore, we investigated whether DesAb-O was able to counteract the neurotoxicity induced by $A\beta_{42}$ species in SH-SY5Y cells, by performing MTT reduction tests and the analysis of oxidative stress by confocal microscopy, in the absence or in the presence of DesAb-O. Finally, by using dot-blot assays and sandwich-ELISA immunoassays, we monitored the ability of DesAb-O to specifically identify $A\beta_{42}$ oligomers rather than monomers and fibrils.

We have been able to obtain well-resolved $A\beta_{42}$ aggregated species during the ThT aggregation assays, including oligomers and fibrils, with different reactive properties, morphology and cytotoxic effects. Moreover, we found that DesAb-O can significantly prevent mitochondrial dysfunction and the production of reactive oxygen species (ROS) induced by $A\beta_{42}$ oligomers, rather than monomers and fibrils. Finally, we demonstrated that DesAb-O can discriminate oligomers from monomers and fibrils, especially at lower concentration.

These evidences strongly suggest that the use of DesAb-O holds great promise for improving the early diagnosis of AD and for a possible future therapeutic application due to its protective capabilities (21).

EXPERIMENTAL PROCEDURES

ThT aggregation assay (6) – The $A\beta_{42}$ aggregation process was monitored by performing a ThT aggregation assay, as previously reported

(24). Briefly, the lyophilised peptide (Bachem) was dissolved in 100% hexafluoro-2-isopropanol (HFIP) to obtain a monomeric form, followed by evaporation under nitrogen flux. Subsequently, the peptide was resuspended in PBS, resulting in a final concentration of 10 µM. For visualisation of the emerging β-sheets in $A\beta_{42}$, samples were added with a final concentration of 25 µM ThT, gently vortexed and pipetted into no binding surface black 96-well plates (Grenier Bio-One, Frickenhausen, Austria) in quadruplets. The plate was read in a BioTek Synergy™ H1 Hybrid Multi-mode reader (Agilent, Santa Clara, United States) at 37 °C. The excitation and emission wavelengths were set to 440 and 485 nm, respectively. Buffer-only values were not subtracted from the sample readings but shown in the final graph. Readings were taken every 2 min. The data were plotted using GraphPad Prism version 9.3.1 for Windows (GraphPad Software, San Diego, CA, United States). In order to characterise the different type of aggregates formed during the $A\beta_{42}$ aggregation process, we collected $A\beta_{42}$ samples at various timepoints (0, 2, 4, 8, and 24 h, corresponding to T0, T1, T2, T3 and T4) to conduct further experiments (see details below).

Preparation of amyloid β-derived diffusible ligands (ADDLs) – To obtain amyloid β-derived diffusible ligands (ADDLs) the lyophilized peptide was resuspended in anhydrous dimethyl sulfoxide (DMSO) to 5 mM and then diluting in ice-cold F-12 medium to a final concentration of 100 µM. This solution was incubated at 4 °C for 1 day and then centrifuged at 14,000 × g for 10 min (28).

Dot-blot analysis – To characterise the different types of $A\beta_{42}$ aggregates formed during the Aβ aggregation process, 2.0 µl (equivalent to 0.1 µg) of the samples at five different timepoints (0, 2, 4, 8, and 24 h, corresponding to T0, T1, T2, T3 and T4, as described above) were spotted onto a nitrocellulose membrane. Following a 45-min blocking step (1.0% bovine serum albumin, BSA, in TBS/TWEEN 0.1%), the membrane was incubated with 1:15.000 diluted human monoclonal anti-ADDLs (19.3) Ab (Creative Biolabs), 1:1000 diluted rabbit polyclonal anti-amyloid fibrils (OC) Ab (Sigma-Aldrich) and 1:800 diluted mouse monoclonal anti-Aβ (6E10) Ab (Biolegend Way) for 1 h and 30 mins. Subsequently, the membrane was washed three times in TBS-TWEEN 0,1% for 10 mins each and incubated with 1:3000 diluted goat anti-6X His tag (Abcam), goat anti-human (Sigma-Aldrich), or goat anti-rabbit (Abcam) or rabbit anti-mouse (Abcam), all conjugated with horseradish peroxidase (HRP) for 1 h. After three additional washes in TBS-TWEEN 0,1%, the immunolabelled dots were detected using a Super-SignalWest Dura (Pierce) ImageQuant™ TL software (GE Healthcare UK Limited version 8.2) as previously reported (21).

In a set of experiments, sandwich dot-blot analysis of $A\beta_{42}$ oligomers collected after 8 h of incubation was performed. The capture Abs, 6E10 and DesAb-O, were spotted onto nitrocellulose membranes (2 µl corresponding to 0.01 mg/ml) for 6E10 and 20 µM, 10 µM, 5 µM, 1 µM for DesAb-O, respectively. The membranes were incubated with solutions containing 1 µM $A\beta_{42}$ oligomers and ADDLs. Finally, the membranes were probed with the detection Ab 6E10 and the proper secondary Ab, as described above.

STED microscopy – $A\beta_{42}$ aggregates collected at different timepoints (0, 2, 4, 8, and 24 h, corresponding to T0, T1, T2, T3 and T4, as described above) were spotted on a glass coverslip for 30 min. Then, the samples were blocked with 1x casein for 30 min, washed with PBS, and incubated with 1:500 diluted 19.3, 1:800 diluted 6E10 or 1:800 diluted OC primary Abs for 1 h and 30 min. After washing with PBS, the samples were incubated with 1:500 diluted Alexa Fluor 488-conjugated anti-human, 514-conjugated anti-mouse and 514-conjugated anti-rabbit secondary Abs. Fluoromount-G™ (Fisher Scientific) was used as mounting medium. STED xyz images (i.e., z-stacks were acquired as previously reported (21) at 0.1 µm intervals along 3 directions: x, y, and z axes) in bidirectional mode with a Leica SP8 STED 3X confocal microscope system equipped with a Leica HC PL APO CS2 100x/1.40 oil STED White objective. Alexa Fluor 514 was excited with a 510 nm-tuned WLL and emission collected from 532 to 551 nm. Frame sequential acquisition was applied to avoid fluorescence overlap. A gating between 0.3 to 6 ns to avoid collection of reflection and autofluorescence was applied. 650 nm pulsed depletion laser was used for Alexa Fluor 514 excitation. Collected images were de-convolved with Huygens Professional software version 18.04

(Scientific Volume Imaging B.V., Hilversum, The Netherlands) and analysed with Leica Application Suite X (LAS X) software (Leica).

Cell culture – Authenticated human SH-SY5Y neuroblastoma cells were purchased from A.T.C.C. and cultured as previously reported (21) in Dulbecco's modified Eagle's medium (DMEM), F-12 Ham with HCO_3 (1:1) supplemented with 10% foetal bovine serum (FBS), 1.0% L-glutamine and 1.0% penicillin and streptomycin solution (Sigma-Aldrich). Cells were maintained in a 5.0% CO_2 humidified atmosphere at 37 °C and tested to ensure that they were free form mycoplasma contamination.

MTT reduction assay – To assess the cytotoxicity of Aβ aggregates formed during the Aβ aggregation process, a 3-(4,5-dimethyltohiazol-2-yl)-2,5-diphenyltetrazolium bromide (MTT) reduction assay was conducted. Briefly $Aβ_{42}$ species collected at different timepoints (0, 2, 4, 8 and 24 h, corresponding to T0, T1, T2, T3 and T4, as described above) were added for 24 h to culture medium of SH-SY5Y cells at a concentration of 0.5 μM (monomer equivalents). In another set of experiments, we performed an MTT test with decreasing concentrations (1 μM, 0.5 μM, 0.25 μM, 1 nM, 0.5 nM, 0.25 nM and 1 pM) of Aβ aggregates obtained after 8 h of incubation (T3). In another set of experiments, Aβ oligomers obtained after 8 h of incubation (T3) were pre-incubated for 1 h at 37 °C under gentle shaking at a concentration of 0.5 μM with increasing concentrations (0.5, 1 and 1.5 μM) of DesAb-O, corresponding to 1:1, 1:2 and 1:3 molar ratio between oligomers and DesAb-O. In all experiments, the cells were also treated with ADDLs at 1 μM concentration (monomer equivalents), as positive control. The solutions were then added to the extracellular medium of SH-SY5Y cells. After treatment, the cell culture medium was removed, cells were washed in PBS and the MTT solution was added to the cells for 4 h. The formazan product was solubilised with cell lysis buffer (20% sodium dodecyl sulphate (SDS), 50% N, N-dimethylformamide, pH 4.7) for 1 h. The absorbance values of blue formazan were determined at 595 nm. MTT tests were achieved using Microplate Manager® Software (Biorad, CA, USA). Cell viability was expressed as the percentage of MTT reduction in treated cells as compared to those untreated (taken as 100%), or to those treated with $Aβ_{42}$ species in the absence of Abs, as previously reported (21).

Measurements of intracellular ROS production – $Aβ_{42}$ oligomers obtained after 8 h of incubation (T3) were pre-incubated for 1 h at 37 °C at 0.5 μM (monomer equivalents) in the absence or presence of DesAb-O at an equimolar ratio between oligomers and Ab. Then, the solutions were added to the extracellular medium of SH-SY5Y cells seeded on glass coverslips for 1 h. The 2′,7′-dichlorodihydrofluorescein diacetate (CMH_2DCFDA, Thermo Fisher Scientific) probe was used to detect and quantify intracellular levels of hydrogen peroxide as a ROS marker. Briefly, the cells were loaded with 5 μM CM-H_2DCFDA in the last 15 min of treatment. H_2O_2 (800 μM) was used as a positive control. The emitted fluorescence was detected at 488 nm excitation line by TCS SP8 scanning confocal microscopy system (Leica Microsystems, Mannheim, Germany), equipped with an argon laser source. A series of 1-μm-thick optical sections (1024 × 1024 pixels) was taken through the cell depth for each sample using a Leica Plan Apo 63× oil immersion objective, and all sections were projected as a single composite image by superimposition. The confocal microscope was set at optimal acquisition conditions, e.g. pinhole diameters, detector gain and laser powers. Settings were maintained constant for each analysis. Images were then analysed using the ImageJ (NIH, Bethesda, MD, USA) software (Rasband 1997–2018). The fluorescence intensities were expressed as the percentage of that measured in untreated cells (taken as 100%) as previously reported (21).

Sandwich-ELISA assay – For the sandwich-ELISA assay, 1 μM of DesAb-O was loaded onto a 96-well Maxisorp ELISA plate under quiescent conditions for 1 h at room temperature (RT). Following three washes in PBS, the plate was blocked by overnight incubation with 5% BSA IgG free at 4 °C. The next day, after six washes with PBS, $Aβ_{42}$ species collected at 0, 8 h and ADDLs oligomers were added at decreasing concentrations (1 μM, 10 nM, 5 nM, 1 nM, 0.1 nM, 10 pM, 5 pM) and kept overnight at 4 °C. ADDLs were used as a positive control. The following day after six washes with PBS, the plate was incubated with 1:4000 6E10 Ab for 2 h at RT. After six washes with PBS-

Tween-20 0.2%, the plate was incubated with 1:5000 anti-mouse secondary Ab for 1 h. Finally, the plate was washed six times with PBS-Tween-20 0.2% and the amount of 6E10 Ab bound to the $A\beta_{42}$ species was quantified using 1-Step Ultra TMB-ELISA Substrate Solution (Termo Fisher Scientifc), according to the manufacturer's instructions. The reaction was stopped by adding 40 µl of H_2SO_4 and the absorbance was measured at 450 nm using a CLARIOstar plate reader (BMG Labtech), as previously reported (21).

Statistical analysis – All data were expressed as means ± standard error of mean (S.E.M). Comparisons between the different groups were performed by ANOVA followed by Bonferroni's post comparison test. A P-value less than 0.05 was considered to be statistically significant.

RESULTS

Characterisation of $A\beta_{42}$ aggregates with ThT assay, dot blot assay and STED microscopy – In order to follow the $A\beta_{42}$ aggregation process overtime, we performed a Thioflavin T (ThT) assay, monitoring the fluorescent emission of the ThT, a widely recognised dye known for its binding to assembling amyloid aggregates (29-31). In this experiment, sample of $A\beta_{42}$ monomers at 10 µM was mixed with 25µM ThT, incubated at 37 °C and ThT fluorescence was monitored at 482 nm over a span of 24 h. The progressive increase of the ThT fluorescent signal provides insight into β-sheets formation. Concomitantly, we collected aliquots of the reaction solution at different timepoints (0, 2, 4, 8 and 24 h, corresponding to T0, T1, T2, T3 and T4) in order to characterise the reactive properties and the morphology of the species formed during the aggregation process. We took advantage of dot blot assay and super resolution STED microscopy coupled with conformation-sensitives Abs able to distinguish specific $A\beta_{42}$ aggregate conformations. In particular, we used the anti-ADDLs 19.3 Ab (32) and the anti-amyloid fibrils OC Ab (33). As controls, we used the 6E10 Ab, which binds to the N-terminus of $A\beta_{42}$ peptides without distinguishing between different conformations.

At T0 (0 h) we found a higher ThT signal compared to the control (sample with ThT in the absence of $A\beta_{42}$) (***Figure 1A***), with only a minimal positivity for 19.3 Ab and none for OC Ab in the dot blot assay and STED images (***Figure 1B and C***). After 2 h of incubation (T1), we observed an increase in ThT fluorescence, indicating the formation of aggregated species (***Figure 1A***), that appeared positive for 19.3 Ab and to a lesser extent for OC Ab (***Figure 1B and C***). At T2 (4 h), the ThT fluorescent signal further increased (***Figure 1A***), as well as the positivity for 19.3 Ab and only a minor signal for OC Ab (***Figure 1B and C***). After 8 h (T3), we found the exponential phase of the sigmoidal curve and a sharp increase in ThT fluorescent signal (***Figure 1A***). Concurrently, strong positivity with 19.3 Ab and the presence of numerous small, globular species in STED images (***Figure 1B and C***) indicated the highest concentration of oligomers. We also noticed a positivity for OC Ab (***Figure 1B and C***), indicating the formation of few fibrillary species. At the end of the aggregation process, (24 h, T4), the ThT curve reached a plateau (***Figure 1A***), suggesting the presence of amyloid fibrils and the end of new aggregate formation. Dot blot assays and STED images showed positivity for OC Ab together with the presence of fibrillary elongated species and only a minor presence of oligomers (***Figure 1B and C***). As control, 6E10 Ab exhibited positivity for each type of species, indicating the proper loading and the progressive maturation of $A\beta_{42}$ fibrils.

$A\beta_{42}$ oligomeric species obtained after 8 hours of incubation exhibit high toxicity – Then, we investigated the toxicity of the various $A\beta_{42}$ aggregates generated during the aggregation process, taking advantage of the MTT reduction test, a widely used method to evaluate cell viability by analysing their mitochondrial status. Indeed, viable cells with active metabolism convert MTT into a purple coloured formazan product (***Figure 2A***) with an absorbance maximum near 570 nm. When cells die, they lose the ability to convert MTT into formazan, making colour formation a practical and convenient marker exclusive to viable cells. In this experiment, $A\beta_{42}$ species collected at different timepoints (T0-T4) were added to the extracellular medium of SH-SY5 cells for 24 h. Our findings reveal that $A\beta_{42}$ species formed at T0, mostly composed of the monomeric form, did not significantly reduce cell mitochondrial activity (16 ± 6%) as compared to untreated cells, taken as 100% (***Figure 2B***). In contrast, from T1 (2 h) we observed a progressive reduction of cell viability (34 ± 4%) which became significant at T2 (4 h) (50

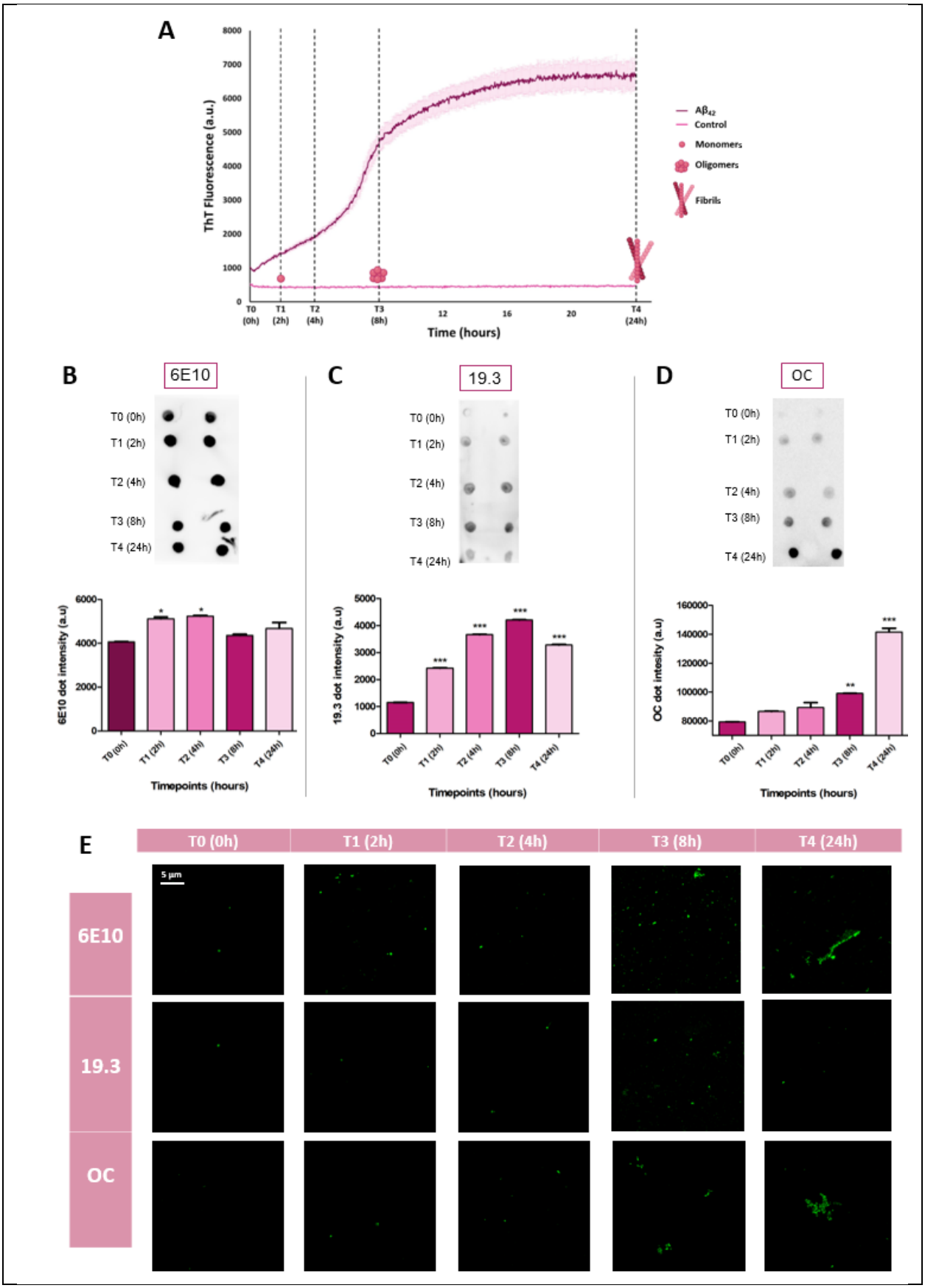
A
ThT Fluorescence (a.u.)
Time (hours)
Aβ42
Control
Monomers
Oligomers
Fibrils
B
6E10
C
19.3
D
OC
T0 (0h)
T1 (2h)
T2 (4h)
T3 (8h)
T4 (24h)
6E10 dot intensity (a.u)
19.3 dot intensity (a.u)
OC dot intesity (a.u)
Timepoints (hours)
E
T0 (0h)
T1 (2h)
T2 (4h)
T3 (8h)
T4 (24h)
5 µm
6E10
19.3
OC

Figure 1: Characterisation of $A\beta_{42}$ aggregates with ThT assay, dot blot and STED microscopy. **A)** Monomeric $A\beta_{42}$ was incubated in PBS at 10 µM with 25 μM thioflavin T (ThT) dye. The plate was read in a BioTek Synergy™ H1 Hybrid Multi-mode reader (Agilent, Santa Clara, United States) at 37 °C. The excitation and emission wavelengths were set to 440 and 485 nm, respectively. Buffer-only values were not subtracted from the sample readings but shown in the final graph. Readings were taken every 2 min. Data were plotted using GraphPad Prism version 5.00 for Windows (GraphPad Software, San Diego, CA, United States). Time points were collected at 0, 2, 4, 8 and 24 h (corresponding to T0, T1, T2, T3 and T4) to perform a characterization of $A\beta_{42}$ aggregates. **B-C)** Dot blot analysis and quantification of $A\beta_{42}$ samples collected at different timepoints. Samples of different $A\beta_{42}$ species were deposited (2 µl/spot) onto a nitrocellulose membrane and detected with the indicated antibodies (Abs). Membranes were incubated with 6E10 (**B**), 19.3 (**C**) and OC (**D**) primary Abs. The dot blot incubated with the 19.3 Ab showed the presence of oligomeric species since the early stage of the aggregation (2 h and 4 h) with the maximum amount reached at 8 h, consistent with the ThT assay showing the exponential phase at 8 h. From the dot blot obtained with the OC Ab, we can see an increase of the dots intensity at 24 h, in line with the aggregation assay showing the reaching of the plateau due to the fibrils formation. Experimental errors are S.E.M. (n = 2). Samples were analysed by One-way ANOVA test followed by Bonferroni's multiple-comparison test relative to their respective time 0 h (*$P < 0{,}05$, **$P < 0.01$, and ***$P < 0.001$). **E)** STED microscopy images and visualisation of $A\beta_{42}$ samples collected at different timepoints. Samples of different $A\beta_{42}$ species were immunolabeled with 6E10, 19.3 and OC Abs. The STED microscopy images are perfectly in line with the dot blot assay results, showing the presence of oligomers since the initial stage of the aggregation $A\beta_{42}$ process as represented in T0 (0 h), T1 (2 h) and T2 (4 h) of 19.3 Abs images. At T4 (24 h), the presence of fibrils is proved by the OC Abs signal being perfectly in line with aggregation assay and dot blot assay results.

± 2%) and reached its peak at T3 (8 h) (58 ± 3%), in which the solution mostly consists of oligomeric species. Finally, at T4 (24 h), we observed minor toxicity with respect to T3 and T2, even if fibrils generated a significant reduction of cell viability (41 ± 4%) (***Figure 2B***). These findings suggest that after 8 h of incubation (T3), the $A\beta_{42}$ oligomers are the most toxic species and thus are most relevant to investigate. Therefore, to delve more into their ability to induce toxicity, we conducted a dose-dependent MTT assay. Different concentrations (ranging from 1 µM to 1 pM) of the aggregates formed at T3 were added to the extracellular medium of SH-SY5Y cells for 24 h. ***Figure 2C*** illustrates that oligomers caused significant mitochondrial dysfunction at 0.5 and 1 µM (reduction of 33 ± 3% and 51 ± 2%, respectively).

With the aim to neutralise cell dysfunction, we assessed whether a sdAb, named DesAb-O, could mitigate the neurotoxic effects induced by $A\beta_{42}$ oligomers. To this purpose, oligomeric species generated after 8 h of incubation (T3) were pre-incubated at 0.5 µM (monomer equivalents) with increasing concentration (0.5 µM, 1 µM, 1.5 µM) of DesAb-O, corresponding to 1:1, 1:2 and 1:3 molar ratio between oligomers and Ab for 1 h at 37 °C under gentle shaking. The solutions were then added to the extracellular medium of SH-SY5Y cells for 24 h. Our results showed that DesAb-O can significantly inhibit oligomer-induced mitochondrial dysfunction only at 1:3 molar ratio, showing no adverse effect on neuronal viability when administered alone (increase of MTT reduction of 12%± 1% with respect to the oligomers alone; ***Figure 3A***).

To further study the protective effect of DesAb-O, we evaluated its ability to prevent oxidative stress induced by $A\beta_{42}$ oligomers in SH-SY5Y cells, taking advantage of confocal microscopy and the CMH_2DCFDA fluorescent probe, a common and useful indicator for ROS in cells. This indicator passively diffuses into cells, where its acetate groups are cleaved by intracellular esterases. Subsequent oxidation yields a fluorescent adduct that is trapped inside the cell, thus facilitating long term studies (***Figure 3B***). Briefly, $A\beta_{42}$ oligomers (T3) were pre-incubated at 0.5 µM (monomer equivalents) with DesAb-O at 1:1 molar ratio between oligomers and DesAb-O for 1 h at 37 °C under gentle shaking. The solutions were then added to the extracellular medium of SHSY-5Y cells for 1 h. Our findings revealed that $A\beta_{42}$ oligomers are able to induce a sharp increase in ROS production (278 ± 7%, compared to the untreated cells taken as 100%; ***Figure 3C***). As a positive control, we also treated the cells with 800 µM H_2O_2. Notably, DesAb-O showed a strong ability to reduce the oxidative stress induced by the oligomers, leading to a significant reduction of the ROS production (151 ± 9% with respect to the oligomers; ***Figure 3C***).

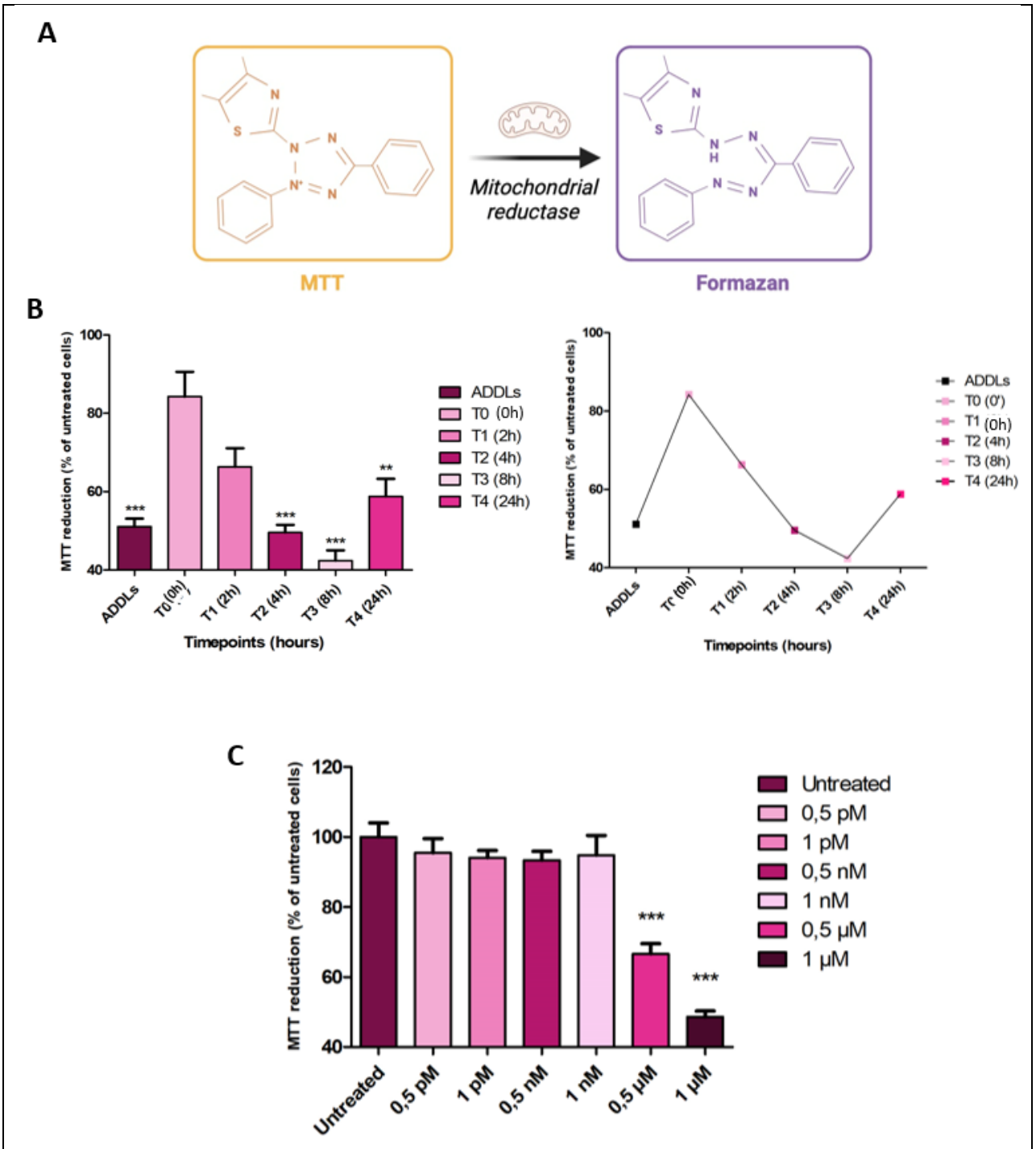

Figure 2: Aβ42 oligomeric species obtained after 8 hours of incubation exhibit high toxicity. **A)** Graphic representation of MTT reaction obtained with Biorender. **B)** MTT reduction in SH-SY5Y cells treated for 24 h with various $A\beta_{42}$ aggregates (1 µM) obtained at different timepoints, denoted as T0 (0 h), T1 (2 h), T2 (4 h), T3 (8 h) and T4 (24 h). ADDLs were used as a positive control. The plot with lines evidences the decrease of vitality and the direct correlation with aggregation time, with a recover of the cells viability at T4 (24 h) linked to the decreased number of oligomers. **C)** MTT reduction in SH-SY5Y cells treated for 24 h with $A\beta_{42}$ aggregates obtained after 8 h of incubation (T3) in a dose-dependent manner. Experimental errors are S.E.M. (n = 3). Samples were analysed by One-way ANOVA followed by Bonferroni's multiple-comparison test relative to untreated cells (**P<0.01,***P<0.001).

DesAb-O binds with high selectivity to oligomeric form of Aβ42 rather than monomeric and fibrillar form – To examine the binding of DesAb-O to oligomers, we performed a sandwich dot blot assay. Briefly, decreasing concentrations of DesAb-O (varying from 20 to 1 µM) were spotted onto a nitrocellulose membrane (2.0 µl), that was then incubated with 1 µM oligomers (T3) or ADDLs. As a positive control, 0.01 mg/ml of 6E10 Ab was also used. ***Figure 4A*** reveals that both membranes showed a sufficient 6E10 intensity, indicating a proper loading of species. Furthermore, membranes treated with T3 oligomers reveal that DesAb-O is able to bind to these species up to a concentration of 5 µM, which is also the case for ADDLs.

To further elucidate this specific binding to oligomers with a more sensitive test, we conducted a sandwich-ELISA assay. After treating the plate with 1 µM of DesAb-O for 24 h, various $A\beta_{42}$ species obtained at different timepoints (T0-T4) were added to the plate. The next day, the plate was first incubated with 1:4000 diluted 6E10 Ab and later with 1:5000 respective secondary Ab. Our results demonstrated that DesAb-O binds with highest affinity to the oligomers (T3), while also binding to monomers (T0; ***Figure 4B***). To delve further into the sensitivity and specificity, we investigated the binding of DesAb-O to oligomers as well as monomers in a dose-dependent manner. After treating the ELISA-plate with different concentrations of $A\beta_{42}$ species (ranging from 10 nM to 5 pM), our findings demonstrate a high sensitivity and specificity of DesAb-O (***Figure 4C***). In particulat DesAb-O was found to detect the oligomers at low concentrations (10 and 5 pM) with respect to monomers (***Figure 4C***).

DISCUSSION

Alzheimer's disease (AD) is a neurodegenerative disorder affecting 55 million people worldwide, highlighting the urgent need for advancement in early detection methods and therapeutic interventions (2). In the past, $A\beta_{42}$ fibrils were considered the primary cause of neuronal damage and AD pathogenesis. However, multiple experimental evidences conducted in different and independent laboratories revealed that the soluble oligomeric species of the $A\beta_{42}$ are the most toxic agents leading to synapse loss and neurodegeneration, which makes them an attractive therapeutical target (34-36).

Conformation-specific Abs developed by various research groups against differently generated $A\beta_{42}$ oligomers have detected these aggregates in AD brains unlike age-matched healthy individuals (36, 37). Notably, these toxic oligomers are detected in the CSF of AD patients, further underscoring their potential as biomarkers for disease progression (14, 38). Furthermore, single domain antibodies (sdAbs) have been recently identified as promising tools due to their low immunogenicity as well as their high specificity and penetrance in tissues (39). In particular, a rational-designed method to develop sdAbs by *Aprile et al.* paved the way for precise targeting of neurotoxic soluble oligomers associated with AD pathology (24)

In this work we characterised various species of $A\beta_{42}$ by monitoring their aggregation over a time course of 24 h, by using the well-known ThT assay. We revealed the presence of soluble oligomers during the exponential phase of the sigmoidal curve, with fibril formation occurring at the plateau. In line with this, in the 1980s it was already demonstrated that oligomers and fibrils emerged during the exponential and plateau phases, respectively. Consistent with this, recent research by *Aprile et al.* confirmed this result, as they also observed oligomers and fibrils at the respective phases by performing a ThT assay with differently generated $A\beta_{42}$ (24, 40). Other researchers conducted asymmetrical flow field-flow fractionation with multi-angle light scattering detection to monitor $A\beta_{42}$ aggregation (41). Consistent with our findings, they found the presence of oligomers already at early stages of the aggregation process (41). By performing dot blot assay and super resolution STED microscopy with 19.3 Ab, which is directed against oligomers, we observed small, globular and round species, especially at T3, during the exponential phase. Moreover, by using OC Ab, that is directed against fibrils, the aggregates obtained in very late stage of the $A\beta_{42}$ aggregation process exhibited a fibrillar phenotype. Several methods utilised by others to characterise $A\beta_{42}$ species confirm these morphologies. For instance, characterisation conducted by total internal reflection fluorescence microscopy (TIRFM), atomic force microscopy (AFM) and direct stochastic optical reconstruction

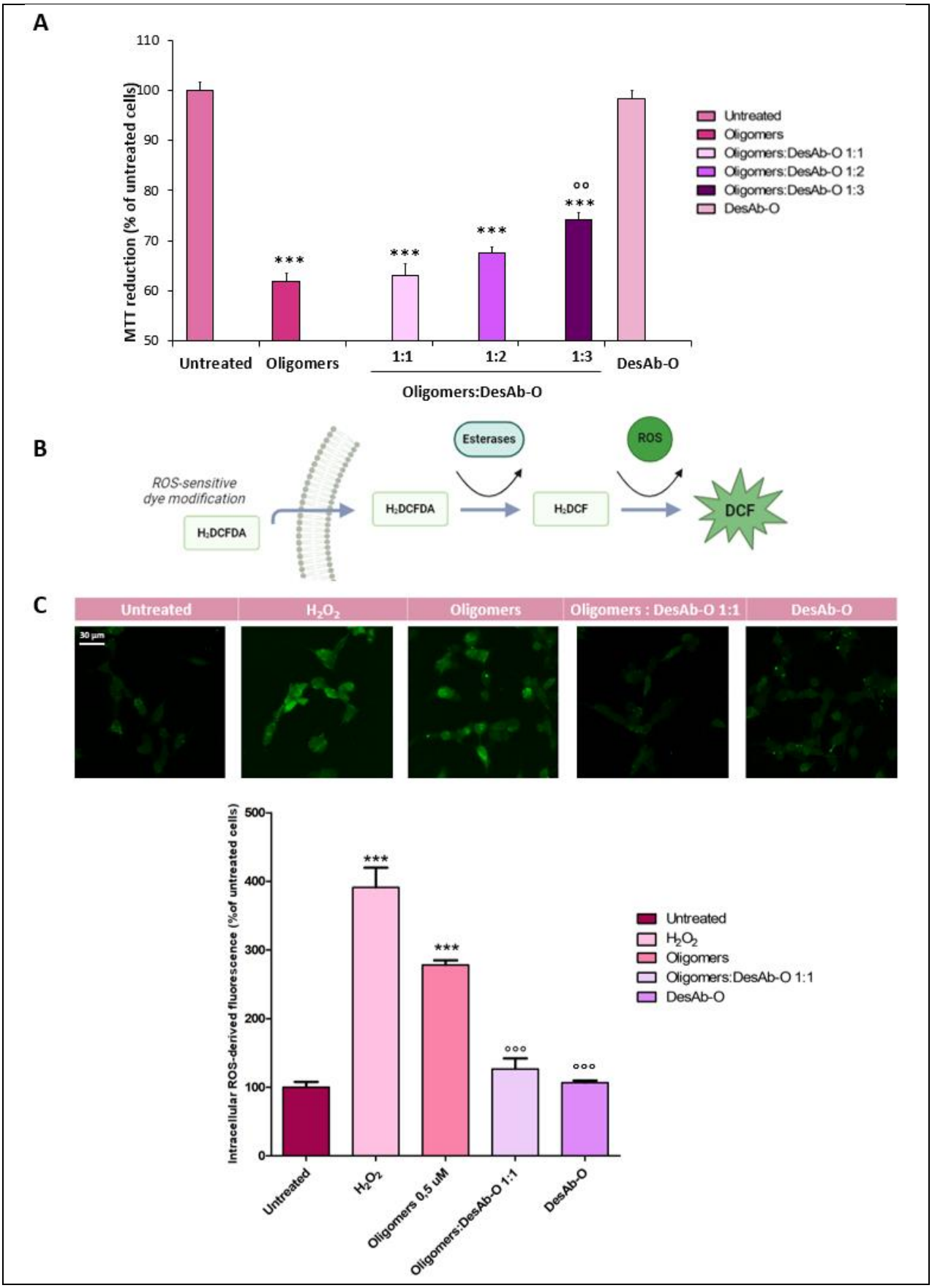
A
MTT reduction (% of untreated cells)
110
100
90
80
70
60
50
***
***
***
oo
***
Untreated
Oligomers
1:1
1:2
1:3
DesAb-O
Oligomers:DesAb-O
Untreated
Oligomers
Oligomers:DesAb-O 1:1
Oligomers:DesAb-O 1:2
Oligomers:DesAb-O 1:3
DesAb-O
B
ROS-sensitive dye modification
H2DCFDA
H2DCFDA
Esterases
H2DCF
ROS
DCF
C
Untreated
H2O2
Oligomers
Oligomers : DesAb-O 1:1
DesAb-O
30 µm
Intracellular ROS-derived fluorescence (%of untreated cells)
500
400
300
200
100
0
***
***
ooo
ooo
Untreated
H2O2
Oligomers 0,5 uM
Oligomers:DesAb-O 1:1
DesAb-O
Untreated
H2O2
Oligomers
Oligomers:DesAb-O 1:1
DesAb-O

Figure 3: DesAb-O mitigates the neurotoxic effects and oxidative stress induced by Aβ42 oligomers. **A)** MTT reduction assay in SH-SY5Y cells treated for 24 h with $A\beta_{42}$ aggregates, obtained after 8 h of incubation (T3), at a concentration of 0.5 μM (monomer equivalents) following a 1 h pre-incubation in the absence or presence of DesAb-O (at 1:1, 1:2, 1:3 molar ratio between oligomers and DesAb-O). DesAb-O alone was also tested as a control. Experimental errors are S.E.M. ($n = 4$). Samples were analysed by One-way ANOVA followed by Bonferroni's multiple-comparison test relative to untreated cells (***$P < 0.001$), or to cells treated with the same $A\beta_{42}$ species without sdAbs (°°$P < 0.01$). **B)** Graphic representation of ROS assay **C)** Cytosolic superoxide can be measured using the CM-H_2DCFDA fluorescent probe. Cells were treated for 1 h with oligomers 0.5 μM, 800 μM H_2O_2 as positive control, and with a 1:1 ratio of oligomers:DesAb-O. SdAbs alone were also tested as a control. In the last 15 mins of the treatment, cells were incubated at 37 °C with 5 μM CM-H_2DCFDA probe. Experimental errors are S.E.M. (n = 3). Samples were analysed by One-way ANOVA followed by Bonferroni's multiple-comparison test relative to cells treated with oligomers 0,5 μM (°°°$P < 0.001$), or to untreated cells (***$P < 0.001$).

microscopy (dSTORM) demonstrated globular and fibrillar morphologies at exponential and plateau phase, respectively (24, 42, 43).

We further evaluated the cytotoxic properties of the various species formed at different timepoints. We found that, after 8 h of incubation at 37 °C, $A\beta_{42}$ oligomers are the most toxic species, with respect to the monomers and fibrils. This confirms the results obtained in other research groups (34, 35). In particular, we observed a dose-dependent increase of toxicity.

With the aim to prevent oligomer-induced cell dysfunction, we examined the protective role of a sdAb, named DesAb-O, which targets a conformational epitope formed by residues 29-36 of $A\beta_{42}$. In particular, we evaluated its ability to prevent mitochondrial dysfunction and ROS production induced by the oligomers. Our findings demonstrated that the pre-incubation of oligomers with DesAb-O strongly prevents their induced mitochondrial dysfunction at 1:3 molar ratio and ROS production at an equimolar concentration, confirming previous findings (21).

Other sdAbs have also been reported to target pathologically relevant $A\beta_{42}$ oligomers. For instance, the development of novel camelid single-chain binding domains (VHHs), named V31-1, which recognises low molecular-weight oligomers specifically. This VHH was able to detect intraneuronal $A\beta_{42}$ oligomers in human brain slices and prevent $A\beta_{42}$-incuded neurotoxicity and even more so, inhibit fibril formation (44). Furthermore, the generation of E1 Ab recognises small oligomers and directs its assembly towards a stable nontoxic conformation, thereby preventing $A\beta_{42}$-induced toxicity *in vitro* (45). Finally, PrioAD13 developed against $A\beta_{42}$ was able to detect oligomers in the blood as well as in the retina of APP/PS1 mice compared to age-matched wild type controls (46). Of note, 24B3, which is a monoclonal Ab with conformational specificity for a toxic conformer of $A\beta_{42}$, detected a higher ratio of toxic conformer to total $A\beta_{42}$ in AD and MCI patients with respect to age-matched controls. In contrast, the difference in total $A\beta_{42}$ was not significant. These findings suggest the diagnostic relevancy of the proportion of toxic $A\beta_{42}$-conformers, rather than the total amount (16).

In order to gain insight into the specificity of DesAb-O, we assessed its ability to bind oligomers with respect to monomers and fibrils by using a sandwich-ELISA assay. We found that DesAb-O targets $A\beta_{42}$ oligomers (T3) with high affinity, even at lower concentrations, showing only minor binding to the monomers. This is in good agreement with previous findings, since DesAb-O is designed to bind to the epitope 29 to 36 of $A\beta_{42}$ (21, 24).

Our study adds to the growing body of evidence supporting the utilisation of sdAbs for targeting toxic oligomers as a promising strategy for AD diagnosis and therapy. However additional research is required to get more insight into the efficacy, specificity and safety for improving early detection and treatment outcomes in AD patients.

CONCLUSION

In our study, we reveal the promising potential of a single-domain antibody (sdAb), called DesAb-O, underscoring its efficiency in both early detection as well as therapeutic intervention. Employing a wide range of biochemical and cell biological techniques, including ThT assay, dot blot, MTT assays, ELISA, STED microscopy and confocal microscopy, we demonstrate the great potential of DesAb-O to identify and neutralise neurotoxic $A\beta_{42}$ oligomers. Our findings collectively underscore the powerful ability of

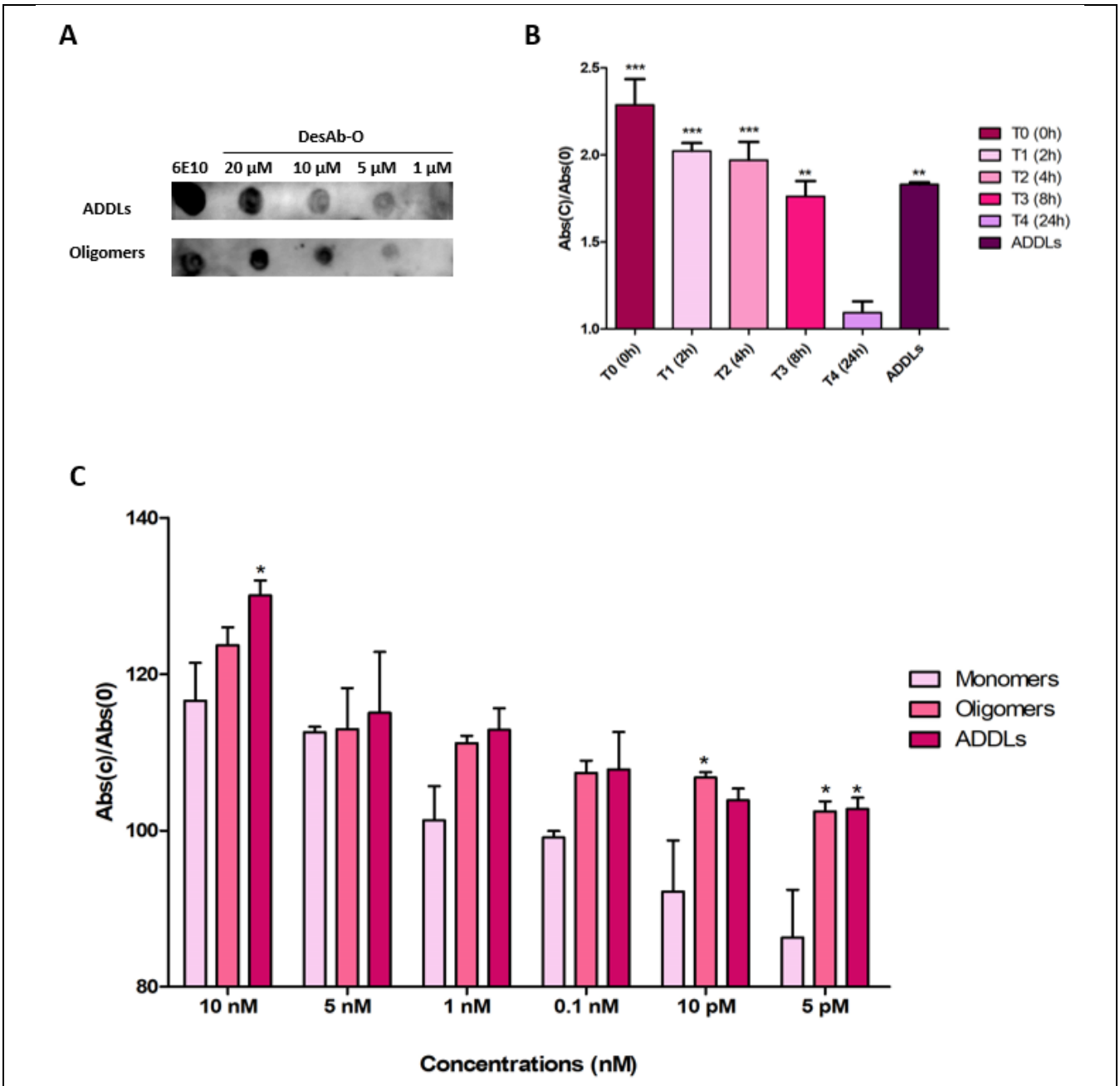

Figure 4: DesAb-O binds with high selectivity to oligomeric form of Aβ$_{42}$ rather than monomers and fibrils. **A)** Representative sandwich dot-blot analysis of Aβ$_{42}$ oligomers collected after 8 h of incubation. The capture Abs, 6E10 and DesAb-O, were spotted onto nitrocellulose membranes (2 µl corresponding to 0.01 mg/ml for 6E10 and 20 µM, 10 µM, 5 µM, 1 µM for DesAb-O, respectively). The membranes were incubated with solutions containing Aβ$_{42}$ oligomers and ADDLs. Finally, the membranes were probed with the detection Ab 6E10. **B)** For sandwich-ELISA assay, 1 µM DesAb-O was immobilised on a 96-well Maxisorp ELISA plate under quiescent conditions for 1 h at RT. The day after different Aβ$_{42}$ species collected at different timepoints (0, 2, 4, 8, 24 h) were loaded into the plate overnight at 4 °C under constant shaking. Experimental errors are S.E.M (n = 3). Samples were analysed by One-way ANOVA followed by Bonferroni's multiple-comparison test relative to 0 µM (**$P < 0.01$, ***$P < 0.001$). **C)** Sandwich-ELISA assay with decreasing concentrations (1 µM, 10 nM, 5 nM, 1 nM, 0.1 nM, 10 pM, 5 pM) of Aβ$_{42}$ species (at 0 h and 8 h, corresponding to the monomers and oligomers, respectively). Samples were adsorbed and quantified by using DesAb-O at 1 µM. ADDLs were used as a positive control. Experimental errors are S.E.M (n = 3). Samples were analysed by Two-way ANOVA (*$P < 0,05$ with respect to the monomer for each concentration).

sdAbs as new promising tools for the improvement of both diagnostic and therapeutic strategies against AD.

Acknowledgments – I would like to thank my daily supervisor Liliana Napolitano and my promotor Roberta Cascella for providing excellent feedback throughout my internship. Furthermore, I would also like to thank the department of Experimental and Clinical Biomedical Sciences for accepting me into their team.

Author contributions – RC and LN conceived and designed the research. LN and IK performed experiments and data analysis. RC provided assistance with STED microscopy. IK wrote the paper. All authors carefully revised and edited the manuscript.

REFERENCES

1. Line Asam. Global Dementia Cases Forecasted to Triple by 2050. 2021:4.
2. World Health Organization . Geneva, Switzerland: World Health Organization; 2021. Fact sheets of dementia [Internet] [cited 2022 Apr 13].
3. Barnett JH, Lewis L, Blackwell AD, Taylor M. Early intervention in Alzheimer's disease: a health economic study of the effects of diagnostic timing. BMC Neurol. 2014 May 7;14:101. doi: 10.1186/1471-2377-14-101.
4. David MW, Mark RC, Ludo, Henrik Z, David MH, Ilse D. Hallmarks of neurodegenerative diseases. Cell. 2023;186(4):693-714.
5. Hardy J, Selkoe DJ. The amyloid hypothesis of Alzheimer's disease: progress and problems on the road to therapeutics. Science. 2002;297(5580):353-6.
6. Kayed R, Sokolov Y, Edmonds B, McIntire TM, Milton SC, Hall JE, Glabe CG. Permeabilization of lipid bilayers is a common conformation-dependent activity of soluble amyloid oligomers in protein misfolding diseases. J Biol Chem. 2004;279(45):46363–6.
7. Benilova I, Karran E, De Strooper B. The toxic Aβ oligomer and Alzheimer's disease: an emperor in need of clothes. Nat Neurosci. 2012;15(3):349–57.
8. Evangelisti E, Cascella R, Becatti M, Marrazza G, Dobson CM, Chiti F, Stefani M, Cecchi C. Binding afnity of amyloid oligomers to cellular membranes is a generic indicator of cellular dysfunction in protein misfolding diseases. Sci Rep. 2016;6:32721.
9. Bigi A, Cascella R, Fani G, Bernacchioni C, Cencetti F, Bruni P, Chiti F, Donati C, Cecchi C. Sphingosine 1-phosphate attenuates neuronal dysfunction induced by Aβ oligomers through endocytic internalization of NMDA receptors. FEBS J. 2023;290(1):112–33.
10. Limbocker R, Cremades N, Cascella R, Tessier PM, Vendruscolo M, Chiti F. Characterization of Pairs of Toxic and Nontoxic Misfolded Protein Oligomers Elucidates the Structural Determinants of Oligomer Toxicity in Protein Misfolding Diseases. Accounts of Chemical Research. 2023;56(12):1395-405.
11. Haass C, Selkoe DJ. Soluble protein oligomers in neurodegeneration: lessons from the Alzheimer's amyloid beta-peptide. Nat Rev Mol Cell Biol. 2007;8(2):101–12
12. Cline EN, Bicca MA, Viola KL, Klein WL. The Aβ oligomer hypothesis: beginning of the third decade. J Alzheimers Dis. 2018;64(s1):S567–610
13. Selkoe DJ. Alzheimer disease and aducanumab: adjusting our approach. Nat Rev Neurol. 2019;15(7):365–
14. Hefti F, Goure WF, Jerecic J, Iverson KS, Walicke PA, Krafft GA. The case for soluble Aβ oligomers as a drug target in Alzheimer's disease. Trends Pharmacol Sci. 2013;34(5):261–6.
15. Savage MJ, Kalinina J, Wolfe A, Tugusheva K, Korn R, Cash-Mason T, Maxwell JW, Hatcher NG, Haugabook SJ, Wu G, Howell BJ, Renger JJ, Shughrue PJ, McCampbell A. A sensitive Aβ oligomer assay discriminates Alzheimer's and aged control cerebrospinal fluid. J Neurosci.2014;34(8):2884–97
16. Murakami K, Tokuda M, Suzuki T, Irie Y, Hanaki M, Izuo N, et al. Monoclonal antibody with conformational specificity for a toxic conformer of amyloid β42 and its application toward the Alzheimer's disease diagnosis. Scientific Reports. 2016;6(1):29038.
17. Karran E, De Strooper B. The amyloid hypothesis in Alzheimer disease: new insights from new therapeutics. Nat Rev Drug Discov. 2022;21(4):306-18.
18. van Dyck CH, Swanson CJ, Aisen P, Bateman RJ, Chen C, Gee M, et al. Lecanemab in Early Alzheimer's Disease. N Engl J Med. 2023;388(1):9-21.

19. Budd Haeberlein S, Aisen PS, Barkhof F, Chalkias S, Chen T, Cohen S, et al. Two Randomized Phase 3 Studies of Aducanumab in Early Alzheimer's Disease. J Prev Alzheimers Dis. 2022;9(2):197-210.
20. Leisher S, Bohorquez A, Gay M, Garcia V, Jones R, Baldaranov D, et al. Amyloid-Lowering Monoclonal Antibodies for the Treatment of Early Alzheimer's Disease. CNS Drugs. 2023;37(8):671-7.
21. Bigi A, Napolitano L, Vadukul DM, Chiti F, Cecchi C, Aprile FA, et al. A single-domain antibody detects and neutralises toxic Aβ(42) oligomers in the Alzheimer's disease CSF. Alzheimers Res Ther. 2024;16(1):13.
22. Muyldermans S. Nanobodies: natural single-domain antibodies. Annu Rev Biochem. 2013;82:775–97.
23. Ackaert C, Smiejkowska N, Xavier C, Sterckx YGJ, Denies S, Stijlemans B, et al. Immunogenicity Risk Profile of Nanobodies. Frontiers in Immunology. 2021;12.
24. Aprile FA, Sormanni P, Podpolny M, Chhangur S, Needham LM, Ruggeri FS, et al. Rational design of a conformation-specific antibody for the quantification of Aβ oligomers. Proc Natl Acad Sci U S A. 2020;117(24):13509-18.
25. Aprile FA, Sormanni P, Perni M, Arosio P, Linse S, Knowles TPJ, et al. Selective targeting of primary and secondary nucleation pathways in Aβ42 aggregation using a rational antibody scanning method. Science Advances. 2017;3(6):e1700488.
26. Sormanni P, Aprile FA, Vendruscolo M. Rational design of antibodies targeting specifc epitopes within intrinsically disordered proteins. Proc Natl Acad Sci U S A. 2015;112(32):9902–7.
27. Sormanni P, Aprile FA, Vendruscolo M. Third generation antibody discovery methods: in silico rational design. Chem Soc Rev. 2018;47(24):9137–57
28. Lambert MP, Barlow AK, Chromy BA, Edwards C, Freed R, Liosatos M, Morgan TE, Rozovsky I, Trommer B, Viola KL, Wals P, Zhang C, Finch CE, Krafft GA, Klein WL. Diffusible, nonfibrillar ligands derived from Abeta1-42 are potent central nervous system neurotoxins. Proc Natl Acad Sci U S A. 1998 May 26;95(11):6448-53.
29. Biancalana M, Koide S. Molecular mechanism of Thioflavin-T binding to amyloid fibrils. Biochimica et Biophysica Acta (BBA) - Proteins and Proteomics. 2010;1804(7):1405-12.
30. LeVine H 3rd. Thioflavine T interaction with synthetic Alzheimer's disease beta-amyloid peptides: detection of amyloid aggregation in solution. Protein Sci. 1993 Mar;2(3):404-10.
31. Soto C, Castaño EM, Frangione B, Inestrosa NC. The alpha-helical to beta-strand transition in the amino-terminal fragment of the amyloid beta-peptide modulates amyloid formation. J Biol Chem. 1995 Feb 17;270(7):3063-7.
32. Savage MJ, Kalinina J, Wolfe A, Tugusheva K, Korn R, Cash-Mason T, et al. A sensitive aβ oligomer assay discriminates Alzheimer's and aged control cerebrospinal fluid. J Neurosci. 2014;34(8):2884-97.
33. Kayed R, Head E, Sarsoza F, Saing T, Cotman CW, Necula M, et al. Fibril specific, conformation dependent antibodies recognize a generic epitope common to amyloid fibrils and fibrillar oligomers that is absent in prefibrillar oligomers. Mol Neurodegener. 2007;2:18.
34. Verma M, Vats A, Taneja V. Toxic species in amyloid disorders: Oligomers or mature fibrils. Ann Indian Acad Neurol. 2015;18(2):138-45.
35. Nimmrich V, Grimm C, Draguhn A, Barghorn S, Lehmann A, Schoemaker H, et al. Amyloid beta oligomers (A beta(1-42) globulomer) suppress spontaneous synaptic activity by inhibition of P/Q-type calcium currents. J Neurosci. 2008;28(4):788-97.
36. Sengupta U, Nilson AN, Kayed R. The Role of Amyloid-β Oligomers in Toxicity, Propagation, and Immunotherapy. EBioMedicine. 2016;6:42-9.
37. Zhang, Y., Chen, H., Li, R. *et al.* Amyloid β-based therapy for Alzheimer's disease: challenges, successes and future. *Sig Transduct Target Ther* **8**, 248 (2023)
38. De S, Whiten DR, Ruggeri FS, Hughes C, Rodrigues M, Sideris DI, et al. Soluble aggregates present in cerebrospinal fluid change in size and mechanism of toxicity during Alzheimer's disease progression. Acta neuropathologica communications [Internet]. 2019 2019/07//; 7(1):[120 p.]
39. Bélanger K, Iqbal U, Tanha J, MacKenzie R, Moreno M, Stanimirovic D. Single-Domain Antibodies as Therapeutic and Imaging Agents for the Treatment of CNS Diseases. Antibodies. 2019;8(2):27.

40. Naiki H, Higuchi K, Hosokawa M, Takeda T. Fluorometric determination of amyloid fibrils in vitro using the fluorescent dye, thioflavin T1. Anal Biochem. 1989;177(2):244-9.
41. Rambaldi DC, Zattoni A, Reschiglian P, Colombo R, De Lorenzi E. In vitro amyloid Abeta(1-42) peptide aggregation monitoring by asymmetrical flow field-flow fractionation with multi-angle light scattering detection. Anal Bioanal Chem. 2009;394(8):2145-9.
42. Young LJ, Kaminski Schierle GS, Kaminski CF. Imaging Aβ(1-42) fibril elongation reveals strongly polarised growth and growth incompetent states. Phys Chem Chem Phys. 2017;19(41):27987-96.
43. Ban T, Goto Y. Direct observation of amyloid growth monitored by total internal reflection fluorescence microscopy. Methods Enzymol. 2006;413:91-102.
44. Lafaye P, Achour I, England P, Duyckaerts C, Rougeon F. Single-domain antibodies recognize selectively small oligomeric forms of amyloid beta, prevent Abeta-induced neurotoxicity and inhibit fibril formation. Mol Immunol. 2009;46(4):695-704.
45. Kasturirangan S, Li L, Emadi S, Boddapati S, Schulz P, Sierks MR. Nanobody specific for oligomeric β-amyloid stabilizes nontoxic form. Neurobiol Aging. 2012;33(7):1320-8.
46. Habiba U, Descallar J, Kreilaus F, Adhikari UK, Kumar S, Morley JW, et al. Detection of retinal and blood Aβ oligomers with nanobodies. Alzheimers Dement (Amst). 2021;13(1):e12193.